

# Lawrence Berkeley National Laboratory

## Recent Work

### Title

A perspective on the electrochemical oxidation of methane to methanol in membrane electrode assemblies

### Permalink

<https://escholarship.org/uc/item/2996f06j>

### Journal

ACS Energy Letters, 5(9)

### ISSN

2380-8195

### Authors

Fornaciari, JC  
Primc, D  
Kawashima, K  
et al.

### Publication Date

2020-09-11

### DOI

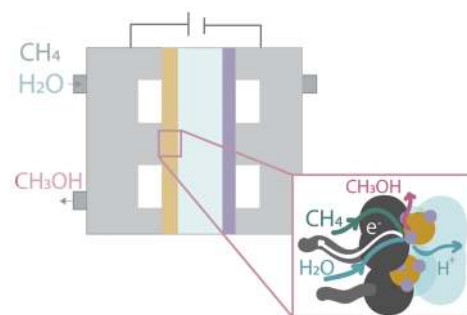
10.1021/acsenergylett.0c01508

Peer reviewed

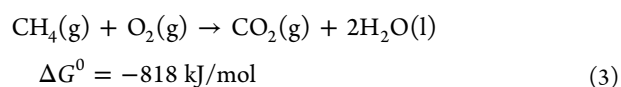
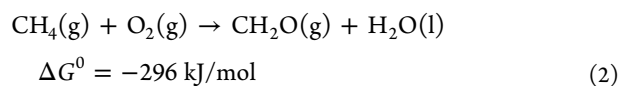
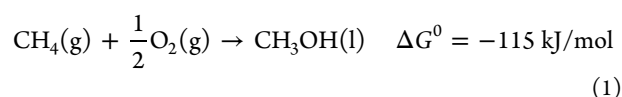
# A Perspective on the Electrochemical Oxidation of Methane to Methanol in Membrane Electrode Assemblies

Julie C. Fornaciari, Darinka Primc, Kenta Kawashima, Bryan R. Wygant, Sumit Verma, Leonardo Spanu, C. Buddie Mullins, Alexis T. Bell,\* and Adam Z. Weber\*

**ABSTRACT:** Direct conversion of methane to methanol has been a long-sought objective. Partial oxidation by thermal catalysis is possible but suffers from a rapid loss in methanol selectivity with increasing methane conversion. More recently, the electrochemical oxidation of methane, using water, rather than oxygen, as the oxidizing agent has been considered in both aqueous electrolyte systems and membrane–electrode assemblies (MEAs). While promising results have been demonstrated using MEAs, the absence of key metrics of system performance make it hard to compare and contrast the results of different investigators. This Perspective examines why MEAs are well-suited for the electrochemical oxidation of methane, defines the metrics for assessing MEA performance, and reviews the progress in the field. An analysis of the challenges to finding suitable electrocatalysts is included with the aim of guiding the search for electrocatalysts that would be both active and selective for the conversion of methane to methanol.



There has been a longstanding interest in identifying processes for the direct conversion of methane to chemicals and fuels because of geographically availability and affordable cost of natural gas.<sup>1,2</sup> The current approach to methane conversion to products is indirect. Methane is steam reformed to synthesis gas, a mixture of CO and H<sub>2</sub>, which is then used to produce products via either methanol or Fischer–Tropsch synthesis. While used today to produce methanol, indirect methane conversion is energetically unattractive for production of transportation fuels and chemicals.<sup>1</sup> We note as well that indirect methane conversion processes (e.g., methanol production) have a high CO<sub>2</sub> footprint because not all of the combusted methane is converted to synthesis gas.<sup>1,2</sup> These considerations have motivated the search for processes that enable the direct oxidation of methane to products, such as methanol or formaldehyde (eqs 1 and 2):



Thermal partial oxidation of methane over a catalyst is difficult to achieve because the Gibbs free energy for the complete combustion of methane to CO<sub>2</sub> and H<sub>2</sub>O (eq 3) is considerably more favorable than that for the partial combustion to methanol and formaldehyde. The high temperatures needed to activate methane create further complications because formaldehyde decomposes to CO and H<sub>2</sub> and methanol can undergo complete combustion. Consequently, high selectivity to formaldehyde and methanol are attainable only at low methane conversions.<sup>3–5</sup> Given the difficulties associated with the thermal partial oxidation of methane, interest has arisen in examining the possibility of oxidizing methane to methanol electrochemically at low temperatures (<150 °C) using water vapor as the oxidant.

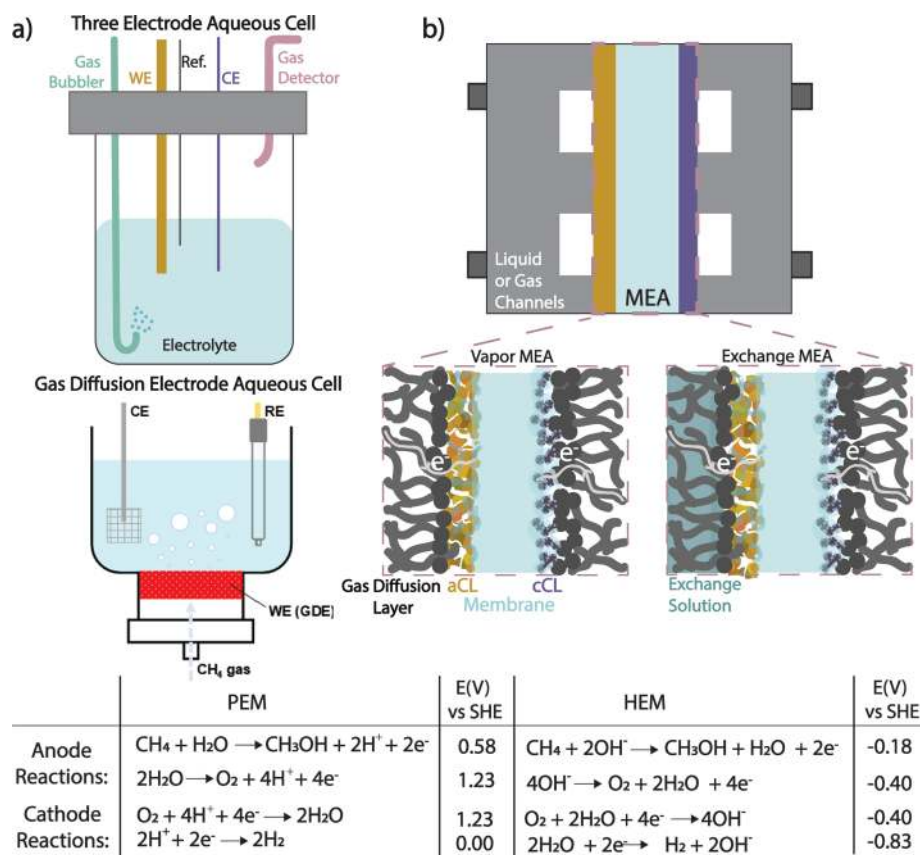
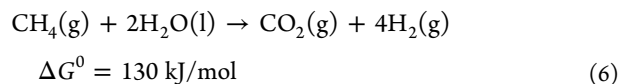
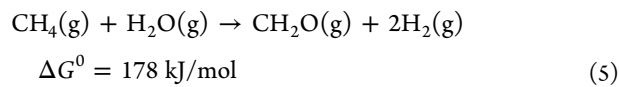
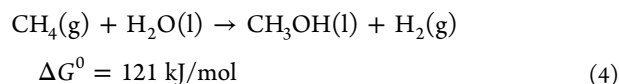


Figure 1. (a) Half-cell set ups for three-electrode and gas diffusion electrode aqueous test cells. (b) Testing MEA cell and (insets) the vapor membrane electrode assembly and the exchange membrane electrode assembly. The desired and potential reactions are shown below for the PEM and HEM cases.

We note that in the case of electrochemical oxidation, using water as the oxidant, the difference in Gibbs free energy for the oxidation of methane to methanol differs from that for the full oxidation to  $\text{CO}_2$  by only 9 kJ/mol (eqs 4–6). This small difference in energy suggests that it may be possible to achieve selectivity to methanol at appreciable conversion levels using an appropriate electrocatalyst. In addition, we are entering an era of more affordable electrical energy produced from renewable sources (e.g., wind and solar), and thus, electrochemical processes are increasingly attractive in terms of cost as well as the potential for lowering the  $\text{CO}_2$  footprint for converting methane to methanol. In this Perspective, we discuss the oxidation of methane to methanol via electrochemical systems and focus on a potential system, a membrane electrode assembly (MEA). The progress in this field is also reviewed. Furthermore, we provide recommendations for selecting electrocatalytic materials for efficient methane-to-methanol conversion.



Different electrochemical systems have been explored for the electrochemical oxidation of methane to methanol. As illustrated in Figure 1, these fall into two main types.<sup>6–20</sup> The simplest is an aqueous electrolyte cell comprising working and counter electrodes (or anode and cathode) immersed in an aqueous electrolyte, as shown in Figure 1a, and, in some cases, may include a third electrode, a reference electrode, to define the working and counter electrodes relative to the electrolyte. The working electrode could also be a gas diffusion electrode, which helps distribute the gas product more efficiently (Figure 1a). Because we can differentiate between the working and the counter electrode, we call these arrangements half-cells.

While aqueous electrolyte cells are useful for rapid evaluation of catalyst activity and selectivity at the working electrode, they cannot achieve the high current densities required for industrial processes ( $200\text{--}1000 \text{ mA/cm}^2$ ). This limitation is because of poor mass transfer of methane dissolved in the electrolyte and low solubility of nonpolar methane in aqueous electrolytes limit the current density to  $<20 \text{ mA/cm}^2$ .<sup>21–23</sup> Product separation is also a concern for aqueous systems because soluble products may undergo complete oxidation.<sup>21</sup> A method for avoiding complete oxidation is to distill these products from the electrolyte.<sup>18</sup> Because methanol has a boiling point of  $65 \text{ }^\circ\text{C}$ ,<sup>24</sup> it can be selectively evaporated from aqueous electrolytes by elevating the aqueous electrolyte temperature ( $\sim 80 \text{ }^\circ\text{C}$ ).<sup>18</sup> However, elevated temperature lowers the methane solubility in aqueous electrolytes and hinders the achievement of high current

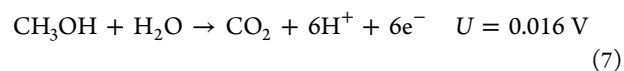
densities. We note that while distillation might be used for exploratory scale studies, this separation method would not be useful in practice because the energy costs for separation would outweigh the fuel value of the products. MEAs, which are illustrated in Figure 1b, offer a means to overcome these limitations.

The MEA architecture can be either fully vapor-fed or have a liquid electrolyte solution (e.g., KOH) fed on one or both sides of the cell, to help regulate the pH and microenvironment around the catalyst.<sup>21,22</sup> The key feature of the MEA architecture is efficient reactant and product transport to and from the catalyst layer and minimal ohmic loss through the membrane. MEAs have been used successfully for fuel cells, electrolyzers, and other energy-conversion technologies and are, therefore, a potentially ideal architecture for the partial oxidation of methane to methanol. As shown in the insets in Figure 1b, the MEA consists of an ionically conducting separator or membrane on one side of which is an anode catalyst layer (aCL) and on the other side is a cathode catalyst layer (cCL). The ion-conducting medium between the two CLs can be a ceramic or a polymer (proton- or anion-conducting), typically  $\sim 100 \mu\text{m}$  thick. Gas-diffusion layers (GDLs) are located on the outside of the CLs to enhance transport of reactants and products as well as facilitate electron transport to and from the CLs. To ensure sufficient transport of ions to and from the catalyst nanoparticles in the CLs, the catalyst nanoparticles are coated with an ionomer, which typically has properties similar to those of the membrane separator. The ionomer also provides a bridge for ion transport to the membrane. The porous CLs and GDLs can be also termed gas diffusion electrodes (GDEs) which can be used in both aqueous and gas fed systems.<sup>21</sup> Note that the complete oxidation of the products can be suppressed by moderating the cell temperature as well as accelerating the mass transport of methanol away from the electrode surface.<sup>6,25,26</sup> Methanol transport can also be enhanced through electrode surface shapes and reactant gas flow.<sup>25–27</sup>

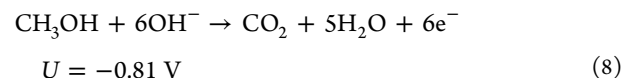
The two most critical parts of an MEA are the catalyst and the ion-conducting medium, i.e., ionomer and membrane. The ionomer and the membrane often set the upper limit on the MEA operating temperature and must exhibit high ionic and electronic conductivity in order to minimize internal impedance of the cell. Both ceramics and polymers have been used as membranes, and each type has its advantages and disadvantages. A ceramic separator must be operated at elevated temperatures, typically  $100\text{--}300 \text{ }^\circ\text{C}$ , in order to exhibit adequate ionic conductivities of  $0.06\text{--}0.2 \text{ S/cm}$ , respectively.<sup>28</sup> Operation at elevated temperatures can be advantageous, because it facilitates the activation of methane; however, preventing full oxidation may be more difficult.<sup>29</sup> A disadvantage of ceramic separators is their brittleness, which can limit their service life because of cracking. On the positive side, though, ceramic separators exhibit minimal product crossover.<sup>28,30</sup> Polymeric membranes can achieve a conductivity of  $\sim 0.1 \text{ S/cm}$  at ambient temperatures, but in order to do so they must be fully hydrated.<sup>29,31</sup> This limits their operating temperature to below  $100 \text{ }^\circ\text{C}$  and requires maintaining the membrane in a hydrated state.<sup>31</sup> Moreover, polymeric membranes generally have a methanol crossover issue, but they could be advantageous in recovering methanol without further oxidation.<sup>32</sup> Typically, proton-exchange membranes (PEMs) (e.g., Nafion and sulfonated poly(ether ether ketone) (SPEEK)) are used because they have higher

stability and are commercially mature.<sup>31,33</sup> A further advantage of PEMs is that they have been optimized for integration into an MEA. This advantage includes well-established methods for fabricating the CLs using PEM ionomer suspensions. Hydroxide-exchange membranes (HEMs) or carbonate-exchange MEAs face stability and low conductivity issues. While researchers can mitigate the conductivity issue by using the exchange-MEA illustrated in Figure 1b, improving the stability and durability of these membranes remains the subject of ongoing research.<sup>34</sup>

Figure 1 lists the reactions that can occur during methane oxidation and their standard potentials (vs standard hydrogen electrode (SHE)) in acidic and basic conditions. In Figure 1, the activation of methane to methanol occurs at the anode where the competing reaction is the oxidation of water if at oxidizing potentials. To minimize the oxidation of methanol, the anode catalyst should have a low activity for the full oxidation for the following reactions



or



for an MEA containing a PEM or a HEM, respectively. Therefore, the selective production of  $\text{CH}_3\text{OH}$  requires that the anode catalyst be much more active for methane than methanol oxidation. We will discuss how these requirements might be met in more detail below.

The reactions listed in the table associated with Figure 1 show that either electrochemical system can be operated in galvanic or electrolytic mode. In the first case (galvanic), the protons produced at the anode react with  $\text{O}_2$  to form  $\text{H}_2\text{O}$ , via the oxygen reduction reaction (ORR), and in the second case (electrolytic), the protons combine and release  $\text{H}_2$ , via the hydrogen evolution reaction (HER), at the cathode. The advantage of operating in the galvanic mode is the cell can generate electricity through the spontaneous reactions and that the cell voltage never reaches highly oxidizing potentials, thereby mitigating the competing reactions at the anode (i.e., the oxygen evolution reaction (OER) requires a potential of  $>1.5 \text{ V}$ ). However, operation in the galvanic mode requires two demanding reactions, the oxidation of methane to methanol at the anode and the ORR at the cathode. The sluggish ORR can limit the maximum current density within the MEA, and the excess  $\text{O}_2$  feed could cross over and further oxidize products at the anode. By contrast, in the electrolytic mode, the HER is a facile reaction and can establish a stable counter electrode potential, providing a clear reference potential to which one can relate the potential for product formation at the anode. Operation in the electrolytic mode requires a supply of electricity to drive the reactions; hydrogen is produced as a high-value byproduct.

*Evaluation of Cell Performance.* In this section, we discuss the metrics for evaluating the performance of an MEA for the case of anodic activation of methane in a PEM electrode assembly (PEMEA). An overall metric for the performance of an MEA is the energy efficiency (EE), which is defined as the amount of methanol produced by the cell compared to the electrical energy consumed. The EE is the product of the Coulombic efficiency (CE) and the voltaic efficiency (VE).

$$EE = VE \times CE \quad (9)$$

Both CE and VE are influenced by the transport of species and the number of reactions occurring at a single electrode as well as the operating conditions of the cell (cell potential, temperature, feed flow rate, etc.). In terms of the transport processes, because there are many fluxes in a MEA, it is important to identify them and understand their origin. As shown in Figure 2 for the PEMEA, water vapor and CH<sub>4</sub> move

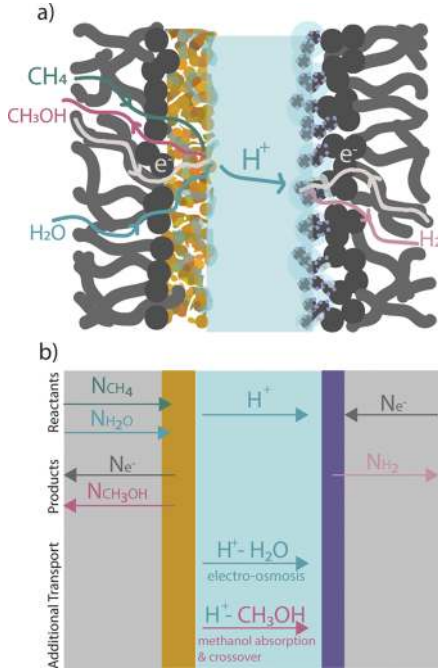


Figure 2. (a) Gas and ion flows through the MEA for electrolytic operation. (b) Fluxes of each individual reactant and product and additional transport mechanisms.

through the aGDL to the aCL under the influence of diffusion and convection, whereas CH<sub>3</sub>OH moves from the aCL in the opposite direction via the same processes. Electrons released in the reaction producing CH<sub>3</sub>OH are transported via the carbon fibers in the aGDL to the anode current collector, whereas protons move from the aCL to the membrane via the connecting ionomer. The protons in the membrane move to the cCL by migration and diffusion because of the gradient in proton concentration and electric field. A part of the total proton flux is associated with water and methanol, and hence, both species move via electro-osmosis toward the cathode. At the cathode side of the membrane, the protons are reduced by electrons flowing from the cathode current collector, resulting in the generation of H<sub>2</sub>, which then is transported through the cCL and cGDL by diffusion and convection. The H<sub>2</sub>O and CH<sub>3</sub>OH associated with protons moving through the membrane are released in the cCL and may diffuse through the cGDL to the cathode flow channel. In the case of CH<sub>3</sub>OH, electro-osmosis contributes to the crossover of this species driven by the concentration gradient in CH<sub>3</sub>OH.

The transport phenomena described above impact the VE, which is a ratio of the thermodynamic potential related to its Gibbs free energy (0.58 V vs SHE), the black dashed line in Figure 3, to the applied cell potential

$$VE \equiv \frac{V_{\text{thermo}}}{V_{\text{applied}}} \quad (10)$$

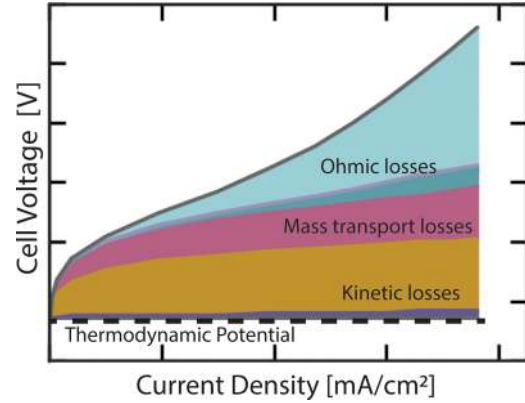


Figure 3. Distribution of overpotentials within the MEA vs current density for an electrolytic cell. The four main components are ohmic losses, mass transport losses, and kinetic losses. Thermodynamic potential is the minimum free energy required to drive the reaction. (Adapted from ref 35.)

Equation 10 is defined for the electrolytic operation; for galvanic mode, the VE is defined as the inverse. As shown in Figure 3, the extra potential required to drive the desired reaction, above the thermodynamic potential, is related to irreversible losses, termed overpotentials. It should be noted that for galvanic operation, similar overpotentials exist, limiting the amount of energy and product generated. As shown in Figure 3, it is clear that the VE decreases nonlinearly with increasing current density. The largest overpotential is related to the reaction kinetics at the anode (the yellow band) and cathode (the purple band) and is often logarithmic with current density (Figure 3). The kinetic losses can be mitigated by increasing the total surface area of the electrocatalysts or developing more efficient electrocatalysts, as discussed below. As noted in Figure 2, the transport of species results in mass transport overpotentials, shown by the pink band in Figure 3, due to concentration changes that occur between the gas channel and the reaction site. These mass transport losses are far from limiting current density and respond more linearly. At limiting-current-density conditions, the mass transport losses will have more rapid increase in voltage with increasing current density. Ion transport through the CLs and the membrane results in ohmic losses. These losses can increase nonlinearly with increasing current density as the degree of hydration in the membrane and ionomer phases change the conductivity of these components. Because membrane and ionomer hydration depend on the transport of water, the ohmic losses are coupled to mass transfer. Both ohmic and mass transport losses can be minimized by changing operating conditions (e.g., raising the temperature) or using thinner membranes; however, there are trade-offs, such as reactant or product crossover, material stability, etc.

The CE is related to how much of the current is used for the methane-to-methanol reaction after accounting for side reactions including possible crossover and reduction of the produced methanol back to methane

$$CE = \frac{i_{\text{methanol}} - i_{\text{crossover}}}{i_T} = FE - \frac{i_{\text{crossover}}}{i_T} \quad (11)$$

With H<sub>2</sub>O as the oxidant,  $\Delta G^0$  for the oxidation of CH<sub>4</sub> to CH<sub>3</sub>OH differs from that for the full oxidation to CO<sub>2</sub> by only 9 kJ/mol, indicating the possibility of achieving selectivity to CH<sub>3</sub>OH at appreciable conversions using an appropriate electrocatalyst.

where  $i_T$  is the total current density and  $i_{\text{methanol}}$  is the partial current density for methanol produced at the anode, determined using Faraday's law. Thus, if all of the produced methanol crosses the membrane and converts to methane, one has designed only an electrochemical methane pump. If there

is no crossover or the methanol does not reduce back to methane (which, typically, has been the case), then CE becomes the same as the Faradaic efficiency (FE). For the methanol reactions, as shown in Figure 1, the FE can be less than 1 because of other reactions at the anode such as the OER.

In eq 11,  $i_{\text{crossover}}$  is not easily measured, and thus, CE is usually evaluated by measuring the total methanol flux and comparing that to the equivalent total flux if all of the current was converted to methanol using Faraday's law

$$CE = \frac{N_{\text{methanol}}}{\frac{i_T}{2F}} \quad (12)$$

where  $N_{\text{methanol}}$  is the total methanol flux leaving the cell in the liquid and gas states for both electrodes and  $F$  is Faraday's

**Table 1. Low-Temperature Electrochemical Methane Oxidation, Experimental Findings<sup>a</sup>**

Products formed	Potential (V)	Current Density (mA/cm <sup>2</sup> )	Electrolyte/Membrane	Temperature (°C)	Electrode (Catalyst/Support)	CH <sub>3</sub> OH Selectivity (CS)/CE	Half or Full Cell	Oxidant	Ref.
CH <sub>3</sub> OH, CO <sub>2</sub>	0.9	4	Sn <sub>0.9</sub> In <sub>0.1</sub> P <sub>2</sub> O <sub>7</sub>	100	V <sub>2</sub> O <sub>5</sub> /SnO <sub>2</sub> -PTFE Anode	88.4% (CS) 61.4% (CE)	Full Cell (PEM)	H <sub>2</sub> O	6
CH <sub>3</sub> OH, CO <sub>2</sub>	---	400	Sn <sub>0.9</sub> In <sub>0.1</sub> P <sub>2</sub> O <sub>7</sub>	50	PdAu/C Cathode	60.0% (CS)	Full Cell (PEM)	O <sub>2</sub>	7
CH <sub>3</sub> OH, CO <sub>2</sub>	---	---	Sn <sub>0.9</sub> In <sub>0.1</sub> P <sub>2</sub> O <sub>7</sub>	300	CuO <sub>x</sub> -PdAu/C Cathode	~ 100% (CS)	Full Cell (PEM)	O <sub>2</sub>	8
CH <sub>3</sub> OH,	0.4-0.5	---	Nafion 117	85 (Anode) 80 (Cathode)	Pt/C Cathode	---	Full Cell (PEM)	H <sub>2</sub> O <sub>2</sub>	9
CH <sub>3</sub> OH	0.3	---	6.0 M KOH/Nafion 117	25 (anode) 80 (cathode)	Pd/C Anode, Pt/C Anode, Ni/C Anode	---	Full Cell (HEM)	OH <sup>-</sup>	10
CH <sub>3</sub> OH	---	---	KOH + H <sub>2</sub> O (Catholyte)/Membrane	160	MO <sub>x</sub> Anode (M = Mn, Fe, Ni, Os, or Pt)	---	Full Cell (HEM)	OH <sup>-</sup>	11
CH <sub>3</sub> OH, CO <sub>2</sub>	---	< 10	KOH + H <sub>2</sub> O (Catholyte)/Daramic Anion Exchange Membrane	25-160	MO <sub>x</sub> Anode (M = Ni, Co, Cu, Ag Pt, Au, Ce, Pb, Fe, Mn, Zn or Combinations)	---	Full Cell (HEM)	OH <sup>-</sup>	12
CH <sub>3</sub> OH, HCHO, CO, HCOOH, CH <sub>3</sub> CH <sub>2</sub> OH, CH <sub>3</sub> COOH, CH <sub>3</sub> COCH <sub>3</sub> , CH <sub>3</sub> CHOHCH <sub>3</sub>	2.0	21	1.0 M Na <sub>2</sub> CO <sub>3</sub> + DMF/Ralex AM-PAD Anion Exchange Membrane	40	NiO-ZrO <sub>2</sub> Anode	---	Full Cell (CO <sub>3</sub> EM)	CO <sub>3</sub> <sup>2-</sup>	13
CH <sub>3</sub> OH, CH <sub>2</sub> O, CH <sub>3</sub> CH <sub>2</sub> OH, C <sub>2</sub> H <sub>4</sub> O, C <sub>3</sub> H <sub>8</sub> O, C <sub>3</sub> H <sub>6</sub> O	2.0 vs. Pt	< 10	0.5 M Na <sub>2</sub> CO <sub>3</sub>	RT	Co <sub>3</sub> O <sub>4</sub> -ZrO <sub>2</sub> /CP-Nafion 117 Anode	---	Half Cell (CO <sub>3</sub> EM)	CO <sub>3</sub> <sup>2-</sup>	14, 15
CH <sub>3</sub> OH, HCHO	2.0 vs. SCE	---	0.1 M Na <sub>2</sub> SO <sub>4</sub>	RT	TiO <sub>2</sub> -RuO <sub>2</sub> -V <sub>2</sub> O <sub>5</sub> /PTFE Anode	57% (CE)	Half cell (GDE)	H <sub>2</sub> O (OH <sup>-</sup> )	16
CH <sub>3</sub> OH, HCHO, HCOOH	2.1 vs. SCE	13	0.1 M Na <sub>2</sub> SO <sub>4</sub>	RT	TiO <sub>2</sub> -RuO <sub>2</sub> /PTFE Anode	30% (CE)	Half Cell (GDE)	H <sub>2</sub> O (OH <sup>-</sup> )	17
CH <sub>3</sub> OH	0.75 vs. Ag/AgCl	62	1.0 M KOH	80	Ni(OH) <sub>2</sub> -NiOOH/Ni Foam Anode	---	Half Cell (TEC)	OH <sup>-</sup>	18
CH <sub>3</sub> OH, C <sub>2</sub> H <sub>5</sub> OH	-0.2/0.64 vs. Ag/AgCl (pulsed potential)	---	0.5 M HClO <sub>4</sub>	25	Pd/Graphite Anode	---	Half Cell (TEC)	H <sub>2</sub> O	19
CH <sub>3</sub> OSO <sub>3</sub> H, CH <sub>3</sub> SO <sub>3</sub> H	2.0 vs. SSE (-1.29 vs. RHE)	≤ ~ 4.5	PdSO <sub>4</sub> in 95-98% H <sub>2</sub> SO <sub>4</sub> (ionic catalyst)	80-140	FTO Anode	---	Half Cell (TEC)	H <sub>2</sub> SO <sub>4</sub> , SO <sub>3</sub>	20

<sup>a</sup>Energy efficiency and voltage efficiency were not reported for any of the following experimental results. RT, room temperature; CP, carbon paper; FTO, fluorine-doped tin oxide glass; PEM, proton-exchange membrane; HEM, hydroxide-exchange membrane; CO<sub>3</sub>EM, carbonate-exchange membrane; GDE, gas diffusion electrode system; TEC, three-electrode cell.

constant. Determination of the total flux of methanol and ability to close the overall carbon balance requires measurement of the concentrations in both the gas and liquid exit streams, as well as the volumetric flow rate of these streams. Furthermore, the total volumetric flow rate out of the cell compartments cannot be assumed to be the same as the inlet flow rate because during the course of the reactions the overall gas flux can change, as can water and other species transporting across the membrane (see Figure 2). For this reason, the measurement of the exact flow rate exiting the cell must be known to obtain an accurate measure of the molar flow rate of products. Such a measurement can be accomplished through various flow meters and calibrated devices, provided any condensable constituents are removed or accounted for (e.g., using water traps). This precise measurement is particularly important at high current densities for which a large fraction of the reactants are consumed, because using the inlet flow rate can lead to inaccurate FEs.<sup>36</sup> Similarly, one may also be interested in the residence time of the gases in the cell, which can be obtained by knowing the free volume of the cell and the inlet flow rate. Residence time is typically more important for half-cells than MEAs because the free volume of the latter is mainly in the channels and backing layers and is really only a concern for high conversion rates.

The intricacies highlighted above demonstrate the complexities in determining VE, CE, and EE. These intricacies are further exacerbated by different types of electrochemical evaluations, including sweep voltammetry (cyclic or linear) or chronoamperometry/chronopotentiometry. In particular, sweep studies are transient and do not necessarily allow for steady-state conditions, thereby resulting in perhaps erroneous calculations for VE and CE, especially in terms of product detection and accumulation under steady-state conditions. Consistent, uniform, and detailed protocols that ameliorate the above concerns are required to help advance this difficult field. These recommendations include explicitly stating the voltage (and a reference potential or the counter electrode), the current density, and the duration of the experiments; the voltage and corresponding current density at which the products are obtained; and a complete carbon balance for the entire cell including the flow rate and concentration of each species. Ancillary data such as the high-frequency cell resistance, measured using electrochemical-impedance spectroscopy, and an explicit statement of CE, VE, and EE should be reported to provide comparisons between different cells and catalysts.

*Literature on Electrochemical Methane-to-Methanol Conversion Devices.* Table 1 summarizes the results of published studies reporting the low-temperature electrochemical oxidation of methane to methanol in both MEAs and half-cells (Figure 1), and several review papers have been published that complement the table for other conditions (i.e., higher temperature, various products, etc.).<sup>3-5</sup> It is readily apparent that the performance metrics provided by each set of authors is incomplete, making it difficult to assess the current status of the field. This conclusion is in complete agreement with that reached in a recent review by Mostaghimi et al.<sup>5</sup> For example, only 6 of the 14 articles report both the current density and the voltage at which methanol is detected, and none report the EE. If the cathode voltage is measured relative to a reference electrode and is compensated for the electrolyte resistance, then the voltage at which all reactions occur is known at the anode. This separation of voltage is possible to do for aqueous

electrolyte systems and is shown for the half-cells that are referenced to a specific potential. In the case of MEAs, the cell voltage is composed of many components, as shown in Figure 3, and determining the separate components is nontrivial. Consequently, the total cell voltage is the only basis for comparing one study to another. Because it is impossible to make definitive comparisons of the results reported with different electrochemical cells, we review what has been learned through the literature, emphasizing full-cell MEA devices. The half-cell systems are useful only for assessing the performance of different electrocatalysts.

None of the reports of exchange-MEAs, using either a hydroxide or carbonate solution fed to the cell, have shown good selectivity or efficiency for methanol formation. Moreover, none have realized current densities greater than  $\sim 20$  mA/cm<sup>2</sup>.<sup>9-14</sup> Also, carbonate-exchange-MEAs produced various products besides methanol, including formic acid, formaldehyde, ethanol, ethers, etc.<sup>12-14</sup> These exchange-MEAs have also been used to test catalysts that are not stable in acidic conditions, such as Ni, Co, and Fe. However, a notable limitation of alkaline or hydroxide MEAs is membrane stability.

**In contrast to aqueous electrochemical systems, gas fed membrane electrode assemblies (MEAs) offer opportunities to alleviate mass transport and product collection/separation challenges.**

Gas fed-MEAs for anodic oxidation of methane, using various metal oxides (i.e., V<sub>2</sub>O<sub>5</sub>, CrO, Mn<sub>2</sub>O<sub>3</sub>, Fe<sub>2</sub>O<sub>3</sub>, CoO, and MoO<sub>3</sub>) and metals (i.e., Ru, Pd, Ag, and Au) supported on SnO<sub>2</sub> have been tested at 100 °C.<sup>6</sup> Using a ceramic proton conductor, Sn<sub>0.9</sub>In<sub>0.1</sub>P<sub>2</sub>O<sub>7</sub>, a current density of only 10 mA/cm<sup>2</sup> is achieved. Among the tested materials, V<sub>2</sub>O<sub>5</sub> supported on SnO<sub>2</sub> exhibited the highest methanol selectivity, 88.4%. The concentrations of methanol and carbon dioxide under these conditions were 0.0306% and 0.0040% (reported in terms of the outlet stream makeup), respectively, at a total current of 2 mA/cm<sup>2</sup>; no other species, such as carbon monoxide and oxygen, were detected. With increasing current density ( $\sim 10$  mA/cm<sup>2</sup>), the methanol percent concentration decreased while the carbon dioxide concentration increased, indicating the progressive oxidation of methanol. MEAs with the same ceramic proton conductor, but introducing methane to the cathode side of the cell and using PdAu/C, CuO<sub>x</sub>-PdAu/C, and Pt/C as the electrocatalysts, were examined for methane activation.<sup>7,8</sup> In this configuration, a methanol selectivity of 60% at 400 mA/cm<sup>2</sup> was achieved at 50 °C; however, the methane conversion was only 0.012%. Upon increasing the temperature to 250 °C, the conversion increased to 0.38% but the methanol selectivity decreased to 6.3%.<sup>7</sup> The authors also reported the rate of CO<sub>2</sub> evolution, which for the PdAu/C catalyst was an order of magnitude greater than the rate of methanol formation. At 250 °C, CO<sub>2</sub> and methanol were formed at a rate of 6 and 0.4  $\mu$ mol/h<sup>1</sup>/cm<sup>2</sup>, respectively. As the conversion of methane increased, CO<sub>2</sub> was the principal product formed. Gas fed-, proton conducting-MEAs have shown the most promising results to date for the evolution of methanol. While systems using ceramic separators are able to oxidize methane to methanol, we believe that there is a greater

potential for MEAs based on polymeric proton conductors because they operate at lower temperatures, which should favor methanol formation over complete combustion.<sup>5</sup>

*Current Status and Recommendations on Electrocatalysts.* In all of the work on methane oxidation reported in Table 1, the basis for selecting the electrocatalysts chosen is not well articulated. The most common feature is that many of the materials chosen are known to be active for OER or methanol-to-CO<sub>2</sub> oxidation reaction in either acidic, neutral, or alkaline electrolytes, with the majority in acidic conditions and limited studies with neutral or alkaline ones.<sup>9–17</sup> However, no rationalization is given for why these materials should be active for methane oxidation.

Accurate quantification of the product selectivity and Faradaic efficiencies can be made only when the overall carbon and related mass balances close. More emphasis on reporting these metrics is required.

To help with the search for potential catalysts, it would be very useful to have a theoretical framework to help guide the search. To this end, Arnason et al. calculated the Gibbs free energy of each adsorbed species for electrochemical methane oxidation and oxygen evolution reactions occurring on a number of metal oxides and MX-enes.<sup>25</sup> The two reactions are envisioned to proceed as shown in Figure 4. Both reactions

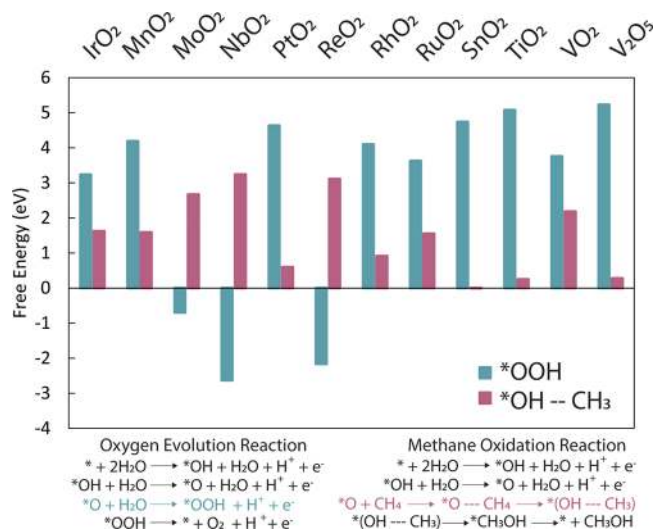


Figure 4. Free energies of various metal oxides for the third step in the water oxidation process and methane activation step. The steps for oxygen evolution and methane activation are shown below. Data from ref 25.

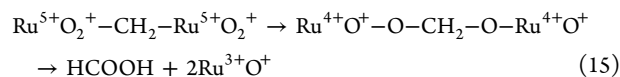
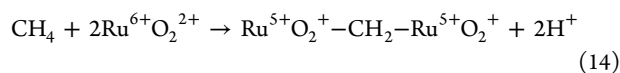
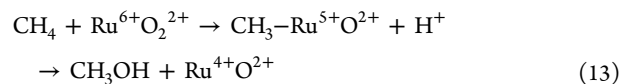
begin with the formation of an adsorbed hydroxide group, which then undergoes dehydrogenation to produce an adsorbed oxygen atom (O\*). Atomic surface oxygen then reacts with water to form a hydroperoxide group, a precursor to O<sub>2</sub>, or with methane to form methanol. Figure 4 shows the calculated free energies for the third step in the OER, the formation of a surface oxyhydroxide (blue), and the activation of methane to form methanol (pink) for a series of metal oxides at open-circuit potential. The smaller the endergonicity

of each step the more easily this step will occur, i.e., the lower the minimum anode potential required for the reaction to proceed. For the preferential formation of methanol over O<sub>2</sub>, the Gibbs free energy for the reaction leading to methanol should be lower than that leading to O<sub>2</sub> via -OOH groups. Accordingly, catalysts such as SnO<sub>2</sub>, TiO<sub>2</sub>, V<sub>2</sub>O<sub>5</sub>, RhO<sub>2</sub>, and PtO<sub>2</sub> would seem to be the most promising candidates for methanol formation. Interestingly, some of the electrocatalysts that have been tested experimentally (in Table 1) align with the predictions shown in this theoretical work (Figure 4).

As noted above, Lee et al. have used V<sub>2</sub>O<sub>5</sub> supported on SnO<sub>2</sub> in a ceramic PEMEA. This system exhibits the highest selectivity (88.4% at 0.03% conversion) to methanol reported to date.<sup>6</sup> During electrocatalysis, partially reduced vanadium species (V<sup>4+</sup>O<sub>2</sub>) act as the active site for generating reactive oxygen species (O<sub>2</sub><sup>•-</sup> and O<sup>•-</sup>) in V<sub>2</sub>O<sub>5</sub>. These species are able to both chemisorb methane and partially oxidize it to methanol. The authors suggest that both methanol and CO<sub>2</sub> are formed at the surface of ceramic, gas fed-MEA anodes, by separate reaction pathways. For methanol, they propose that active oxygen species, such as surface O<sub>2</sub><sup>•-</sup> and O<sup>•-</sup>, may be the primary participants in the partial oxidation of methane to methanol, in agreement with Figure 4. For CO<sub>2</sub>, they propose that highly active oxygen species in the form of an OH\* surface site are responsible for full oxidation of methane to CO<sub>2</sub>, which is also proposed by Yamakata et al. and Heo et al. for various hydrocarbons.<sup>29,37</sup> Accordingly, this hypothesis suggests that CO<sub>2</sub> formation could be suppressed by reducing the amount of OH\* generated during cell operation, thereby improving efficiency. However, they noted that a different support may be needed as SnO<sub>2</sub> may promote full oxidation of methane to carbon dioxide.<sup>6</sup>

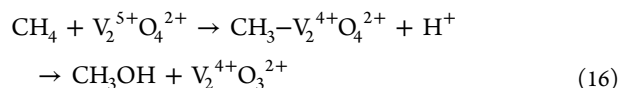
Using consistent, uniform, and detailed experimental protocols (voltage, current density, FE, etc.) will help accurately benchmark materials and advance this difficult field.

Another study that complements the theoretical work is that of Rocha et al., who investigated TiO<sub>2</sub>-RuO<sub>2</sub>/PTFE and TiO<sub>2</sub>-RuO<sub>2</sub>-V<sub>2</sub>O<sub>5</sub>/PTFE for the anodic oxidation of methane to methanol in 0.1 M Na<sub>2</sub>SO<sub>4</sub> into which methane was fed through a GDE.<sup>16,17</sup> Their electrocatalysts achieved a 57% FE toward methanol. Methanol and other byproducts were envisioned to form via two pathways, one involving active oxygen species (e.g., O<sub>2</sub><sup>•-</sup> and O<sup>•-</sup>) and the other involving methane oxidation via a Ru/V redox couple, wherein the transition metals undergo valence transitions.<sup>17</sup> For the latter route, RuO<sub>2</sub> has two active redox couples, Ru<sup>4+</sup>/Ru<sup>6+</sup> and Ru<sup>3+</sup>/Ru<sup>4+</sup>. These redox couples are able to promote the generation of both methanol and formic acid, as shown below:





Conversely,  $V_2O_5$  possesses only one redox couple,  $V^{4+}/V^{5+}$ , which may not generate sufficient electrons to form the double bond needed to generate both formic acid and formaldehyde.



Consequently,  $TiO_2-RuO_2-V_2O_5/PTFE$  can selectively oxidize methane to methanol, whereas  $RuO_2$  bestows electrical conductivity to the GDE on which the catalyst is supported.

### Partial electrochemical oxidation of $CH_4$ to $CH_3OH$ is a difficult problem with limited success in the field.

Considering both experiments and theory, we can envision that a selective electrocatalyst for methane oxidation to methanol should be composed of two phases: a minor phase, having a moderate activity for the first two steps in the OER, and a major phase capable of methane activation. The concept is that oxygen atoms derived from the activation of water on the minority phase would rapidly transfer to the majority phase chosen for its ability to activate methane. By balancing the activation of water and methane, it should be possible to minimize the formation of molecular  $O_2$ . The last requirement is that newly formed methanol is rapidly removed from contact with the electrocatalyst in order to prevent its complete oxidation to  $CO_2$ . This might be done by diffusion of the methanol through the membrane of an MEA to the anode side. Because the anode catalyst generates  $H_2$ , it is important the catalyst that facilitates this process not reduce methanol to methane and water.

In addition to composition, catalyst structure can also influence catalyst activity and selectivity. Therefore, the search for potential catalysts for the selective oxidation of methane to methanol should also include efforts on catalyst characterization. This requirement is particularly important for the development of a multiphase-, bifunctional-electrocatalyst. Such a catalyst requires in-depth investigation of the interfaces between its active phases, because these characteristics will control the transport of atomic O species between the phases. Accordingly, proper evaluation of the structural, morphological, and redox properties of the catalyst needed to obtain a complete understanding of how water and methane are activated.

**An electrocatalyst, composed of a minor phase, which shows a moderate activity for the first two steps in the OER, and the major phase, which would help facilitate  $CH_4$  activation coupled with rapid transport of nascent  $CH_3OH$  away from the catalyst, could be used to achieve high  $CH_3OH$  selectivity at high  $CH_4$  conversions.**

Currently, the phase and structure of electrocatalysts are sometimes reported, but further work is required in order to trace back catalyst activity to catalyst structure. Many reports

include basic structural characterization accomplished with X-ray diffraction (XRD). However, reporting the local crystal structure of the catalysts and correlating it to the catalyst's activity has to be considered as well. Further structural characterization will reveal the amorphous or crystalline nature of the material and identify exposed crystal planes. In addition to XRD, various techniques can be employed to gather further information, including Raman spectroscopy, high-resolution transmission electron microscopy, and X-ray photoelectron spectroscopy. For example, catalysts of the same phase that differ in the exposed crystallographic planes may show differences in their activities for methane oxidation and even lead to evolution of different products. For example, studies on iridium oxide catalysts for the OER have shown variations in activities depending on whether the compound is amorphous or crystalline.<sup>38</sup> Likewise Liang et al. have shown that specific facets of  $IrO_2$  are active for methane oxidation.<sup>39</sup> Similar findings have also been demonstrated by Ma et al., who showed that methane oxidation to carbon monoxide depends on specific facets of a platinum catalyst.<sup>15</sup> For bifunctional catalysts, not only differences in the facets exposed by each component but also the interactions between the surfaces of different materials (i.e., coherency of the lattices or the occurrence of mixed oxidation states) may lead to synergistic catalytic effects.<sup>6-8,13-17</sup> It should be noted that bifunctional catalysts may become unstable when operated at high current densities, and therefore, their structure and composition must be assessed after use, as well as prior to use.

*Summary and Conclusions.* The work reported to date on the electrochemical partial oxidation of methane has shown that while this approach is promising, these are still very early days for the field. More active and selective electrocatalysts that minimize the conversion of methanol to undesired byproducts are required. The reported studies show that a high selectivity to methanol at low methane conversion rates is achievable, but the methanol selectivity rapidly decreases as the methane conversion rate increases. These findings are similar to those reported for the thermal oxidation of methane. What is not clear is to what extent the observed trend of methanol selectivity and methane conversion can be altered by proper design of the electrochemical cell, as well as the electrocatalyst. We also note that using water as the oxidant greatly reduces the thermodynamic driving force for the complete oxidation of methane relative to its partial oxidation to methanol.

The published electrochemical studies of methane oxidation have used both aqueous/nonaqueous electrolyte cells (i.e., half-cells) and membrane-electrolyte assemblies, MEAs (i.e., full-cells), the latter of which have distinct advantages. MEAs are capable of achieving the high current densities ( $\gg 100$  mA/cm<sup>2</sup>) needed for a commercially viable technology. Within this paper, we have detailed the factors affecting the performance of these systems, such as the mode of operation, the microenvironment tested (i.e., acidic versus alkaline), and the nature of the membrane (e.g., polymer versus ceramic). The critical metrics, i.e., the EE, CE, and VE, need to be carefully measured and reported in order to have a basis for comparing different electrochemical systems. Electrocatalyst discovery remains the main obstacle within the field, and both experiments and theory suggest that bifunctional catalysts hold the greatest promise. Characterization of intrinsic electrocatalytic material properties, such as the crystal phase structure and the interactions between different metals or phases, are crucial to further understanding the mechanism for methane

activation and selectivity toward methanol. In summary, this Perspective provides an approach for a systematic approach for understanding the issues associated with the development of electrocatalysts and electrochemical systems for the partial oxidation of methane.

## ■ AUTHOR INFORMATION

### Corresponding Authors

**Alexis T. Bell** – *Department of Chemical and Biomolecular Engineering, University of California Berkeley, Berkeley, California 94720, United States; Joint Center for Artificial Photosynthesis, Lawrence Berkeley National Laboratory, Berkeley, California 94720, United States;* [orcid.org/0000-0002-5738-4645](https://orcid.org/0000-0002-5738-4645); Email: [alexbell@berkeley.edu](mailto:alexbell@berkeley.edu)

**Adam Z. Weber** – *Energy Storage and Distributed Resources Division, Lawrence Berkeley National Laboratory, Berkeley, California 94720, United States;* [orcid.org/0000-0002-7749-1624](https://orcid.org/0000-0002-7749-1624); Email: [azweber@lbl.gov](mailto:azweber@lbl.gov)

### Authors

**Julie C. Fornaciari** – *Energy Storage and Distributed Resources Division, Lawrence Berkeley National Laboratory, Berkeley, California 94720, United States; Department of Chemical and Biomolecular Engineering, University of California Berkeley, Berkeley, California 94720, United States*

**Darinka Primc** – *Energy Storage and Distributed Resources Division, Lawrence Berkeley National Laboratory, Berkeley, California 94720, United States; Department of Chemical and Biomolecular Engineering, University of California Berkeley, Berkeley, California 94720, United States;* [orcid.org/0000-0003-2438-526X](https://orcid.org/0000-0003-2438-526X)

**Kenta Kawashima** – *Department of Chemistry and John J. McKetta Department of Chemical Engineering, University of Texas at Austin, Austin, Texas 78712, United States;* [orcid.org/0000-0001-7318-6115](https://orcid.org/0000-0001-7318-6115)

**Bryan R. Wygant** – *Department of Chemistry and John J. McKetta Department of Chemical Engineering, University of Texas at Austin, Austin, Texas 78712, United States*

**Sumit Verma** – *Shell International Exploration and Production Inc., Houston, Texas 77082, United States;* [orcid.org/0000-0001-8365-180X](https://orcid.org/0000-0001-8365-180X)

**Leonardo Spanu** – *Shell International Exploration and Production Inc., Houston, Texas 77082, United States*

**C. Buddie Mullins** – *Department of Chemistry and John J. McKetta Department of Chemical Engineering, University of Texas at Austin, Austin, Texas 78712, United States;* [orcid.org/0000-0003-1030-4801](https://orcid.org/0000-0003-1030-4801)

Complete contact information is available at:

<https://pubs.acs.org/10.1021/acseenergylett.0c01508>

### Notes

The authors declare no competing financial interest.

## ■ ACKNOWLEDGMENTS

The authors acknowledge Shell's New Energies Research and Technology (NERT) and the Energy & Biosciences Institute through the EBI-Shell Program. The authors also acknowledge Dr. Sander van Bavel for a critical review of the manuscript. J.C.F. thanks the National Science Foundation (Grant DGE 1752814) for support. C.B.M. acknowledges the Welch Foundation (Grant F-1436) for their generous continued support. J.C.F., D.P., K.K., C.B.M., A.T.B., and A.Z.W. composed the manuscript, and all authors edited the written work.

## ■ REFERENCES

- (1) Ravi, M.; Ranocchiari, M.; van Bokhoven, J. A. The Direct Catalytic Oxidation of Methane to Methanol-A Critical Assessment. *Angew. Chem., Int. Ed.* **2017**, *56* (52), 16464–16483.

- (2) Zakaria, Z.; Kamarudin, S. K. Direct conversion technologies of methane to methanol: An overview. *Renewable Sustainable Energy Rev.* **2016**, *65*, 250–261.
- (3) Meng, X.; Cui, X.; Rajan, N. P.; Yu, L.; Deng, D.; Bao, X. Direct Methane Conversion under Mild Condition by Thermo-, Electro-, or Photocatalysis. *Chem.* **2019**, *5*, 2296–2325.
- (4) Xie, S.; Lin, S.; Zhang, Q.; Tian, Z.; Wang, Y. Selective Electrocatalytic Conversion of Methane to Fuels and Chemicals. *J. Energy Chem.* **2018**, *27*, 1629–1636.
- (5) Bagherzadeh Mostaghimi, A. H.; Al-Attas, T. A.; Kibria, M. G.; Siahrostami, S. A review on electrocatalytic oxidation of methane to oxygenates. *J. Mater. Chem. A* **2020**, *8* (31), 15575–15590.
- (6) Lee, B.; Hibino, T. Efficient and Selective Formation of Methanol from Methane in a Fuel Cell-Type Reactor. *J. Catal.* **2011**, *279*, 233–240.
- (7) Tomita, A.; Nakajima, J.; Hibino, T. Direct Oxidation of Methane to Methanol at Low Temperature and Pressure in an Electrochemical Fuel Cell. *Angew. Chem., Int. Ed.* **2008**, *47*, 1462–1464.
- (8) Lee, B.; Sakamoto, Y.; Hirabayashi, D.; Suzuki, K.; Hibino, T. Direct Oxidation of Methane to Methanol over Proton Conductor/Metal Mixed Catalysts. *J. Catal.* **2010**, *271*, 195–200.
- (9) Nandeha, J.; Piasentin, R. M.; Silva, L. M. G.; Fontes, E. H.; Neto, A. O.; De Souza, R. F. B. Partial Oxidation of Methane and Generation of Electricity using a PEMFC. *Ionics* **2019**, *25*, S077–S082.
- (10) Santos, M. C. L.; Nunes, L. C.; Silva, L. M. G.; Ramos, A. S.; Fonseca, F. C.; Souza, R. F. B.; Neto, A. O. Direct Alkaline Anion Exchange Membrane Fuel Cell to Converting Methane into Methanol. *ChemistrySelect* **2019**, *4*, 11430–11434.
- (11) Fan, Q. Method for Producing Methanol from Methane. U.S. Patent Application Publication. US 2014/0124381. May 8, 2014.
- (12) Fan, Q. Non-Faradaic Electrochemical Promotion of Catalytic Methane Reforming for Methanol Production. U.S. Patent Application Publication. US 2015/0129430 A1. May 14, 2015.
- (13) Spinner, N.; Mustain, W. E. Electrochemical Methane Activation and Conversion to Oxygenates at Room Temperature. *J. Electrochem. Soc.* **2013**, *160*, F1275–F1281.
- (14) Ma, M.; Oh, C.; Kim, J.; Moon, J. H.; Park, J. H. Electrochemical CH<sub>4</sub> Oxidation into Acids and Ketones on ZrO<sub>2</sub>:NiCo<sub>2</sub>O<sub>4</sub> Quasi-Solid Solution Nanowire Catalyst. *Appl. Catal., B* **2019**, *259*, 118095.
- (15) Ma, M.; Jin, B. J.; Li, P.; Jung, M. S.; Kim, J. I.; Cho, Y.; Kim, S.; Moon, J. H.; Park, J. H. Ultrahigh Electrocatalytic Conversion of Methane at Room Temperature. *Adv. Sci.* **2017**, *4*, 1700379.
- (16) Rocha, R. S.; Reis, R. M.; Lanza, M. R. V.; Bertazzoli, R. Electrosynthesis of Methanol from Methane: The Role of V<sub>2</sub>O<sub>5</sub> in the Reaction Selectivity for Methanol of a TiO<sub>2</sub>/RuO<sub>2</sub>/V<sub>2</sub>O<sub>5</sub> Gas Diffusion Electrode. *Electrochim. Acta* **2013**, *87*, 606–610.
- (17) Rocha, R. S.; Camargo, L. M.; Lanza, M. R. V.; Bertazzoli, R. A Feasibility Study of the Electro-recycling of Greenhouse Gases: Design and Characterization of a (TiO<sub>2</sub>/RuO<sub>2</sub>)/PTFE Gas Diffusion Electrode for the Electrosynthesis of Methanol from Methane. *Electrocatalysis* **2010**, *1*, 224–229.
- (18) Korin, E.; Bettelheim, A.; Frimmet, L.; Laplan, A.; Kadosh, Y. Electrochemical Oxidation of Methane to Methanol. World Intellectual Property Organization. WO 2019/224811 A1. Nov. 28, 2019.
- (19) Scharifker, B.; Yopez, O.; Jesus, J. C. D.; Agudelo, M. M. R. D. Electrocatalyst for the Oxidation of Methane and an Electrocatalytic Process. US5051156A, September 24, 1991.
- (20) O'Reilly, M. E.; Kim, R. S.; Oh, S.; Surendranath, Y. Catalytic Methane Monofunctionalization by an Electrogenated High-Valent Pd Intermediate. *ACS Cent. Sci.* **2017**, *3*, 1174–1179.
- (21) Higgins, D.; Hahn, C.; Xiang, C.; Jaramillo, T. F.; Weber, A. Z. Gas-Diffusion Electrodes for Carbon Dioxide Reduction: A New Paradigm. *ACS Energy Lett.* **2019**, *4*, 317–324.
- (22) Weng, L. C.; Bell, A. T.; Weber, A. Z. Towards Membrane-Electrode Assembly Systems for CO<sub>2</sub> Reduction: A Modeling Study. *Energy Environ. Sci.* **2019**, *12*, 1950–1968.
- (23) Durst, J.; Rudnev, A.; Dutta, A.; Fu, Y.; Herranz, J.; Kaliginedi, V.; Kuzume, A.; Permyakova, A. A.; Paratcha, Y.; Broekmann, P.; Schmidt, T. J. Electrochemical CO<sub>2</sub> Reduction – Critical View on Fundamentals, Materials and Applications. *Chimia* **2015**, *69*, 769–776.
- (24) Ott, J.; Gronemann, V.; Pontzen, F.; Fiedler, E.; Grossmann, G.; Kersebohm, D. B.; Weiss, G.; Witte, C. Methanol. In *Ullmann's Encyclopedia of Industrial Chemistry*; Wiley, 2012.
- (25) Arnarson, L.; Schmidt, P. S.; Pandey, M.; Bagger, A.; Thygesen, K. S.; Stephens, I. E. L.; Rossmeisl, J. Fundamental Limitation of Electrocatalytic Methane Conversion to Methanol. *Phys. Chem. Chem. Phys.* **2018**, *20*, 11152–11159.
- (26) Seidel, Y. E.; Schneider, A.; Jusys, Z.; Wickman, B.; Kasemo, B.; Behm, R. J. Transport effects in the electrooxidation of methanol studied on nanostructured Pt/glassy carbon electrodes. *Langmuir* **2010**, *26* (5), 3569–78.
- (27) Márquez-Montes, R. A.; Collins-Martínez, V. H.; Pérez-Reyes, I.; Chávez-Flores, D.; Graeve, O. A.; Ramos-Sánchez, V. H. Electrochemical Engineering Assessment of a Novel 3D-Printed Filter-Press Electrochemical Reactor for Multipurpose Laboratory Applications. *ACS Sustainable Chem. Eng.* **2020**, *8*, 3896–3905.
- (28) Heo, P.; Kajiyama, N.; Kobayashi, K.; Nagao, M.; Sano, M.; Hibino, T. Proton Conduction in Sn<sub>0.95</sub>Al<sub>0.05</sub>P<sub>2</sub>O<sub>7</sub>-PBI-PTFE Composite Membrane. *Electrochem. Solid-State Lett.* **2008**, *11*, B91.
- (29) Heo, P.; Ito, K.; Tomita, A.; Hibino, T. A Proton-Conducting Fuel Cell Operating with Hydrocarbon Fuels. *Angew. Chem., Int. Ed.* **2008**, *47* (41), 7841–7844.
- (30) Paschos, O.; Kunze, J.; Stimming, U.; Maglia, F. A Review on Phosphate Based, Solid State, Protonic Conductors for Intermediate Temperature Fuel Cells. *J. Phys.: Condens. Matter* **2011**, *23*, 234110.
- (31) Kusoglu, A.; Weber, A. Z. New Insights into Perfluorinated Sulfonic-Acid Ionomers. *Chem. Rev.* **2017**, *117*, 987–1104.
- (32) Li, W.; Manthiram, A.; Guiver, M. D. Acid-Base Blend Membranes Consisting of Sulfonated Poly(Ether Ether Ketone) and 5-Amino-Benzotriazole Tethered Polysulfone for DMFC. *J. Membr. Sci.* **2010**, *362* (1), 289–297.
- (33) Merle, G.; Wessling, M.; Nijmeijer, K. Anion Exchange Membranes for Alkaline Fuel Cells: A Review. *J. Membr. Sci.* **2011**, *377*, 1–35.
- (34) Hickner, M. A.; Herring, A. M.; Coughlin, E. B. Anion exchange membranes: Current status and moving forward. *J. Polym. Sci., Part B: Polym. Phys.* **2013**, *51*, 1727–1735.
- (35) Fornaciari, J. C.; Gerhardt, M. R.; Zhou, J.; Regmi, Y. N.; Danilovic, N.; Bell, A. T.; Weber, A. Z. The Role of Water in Vapor-fed Proton-Exchange-Membrane Electrolysis. *J. Electrochem. Soc.* **2020**, *167*, 104508.
- (36) Ma, M.; Clark, E. L.; Therkildsen, K. T.; Dalsgaard, S.; Chorkendorff, I.; Seger, B. Insights into the Carbon Balance for CO<sub>2</sub> Electroreduction on Cu using Gas Diffusion Electrode Reactor Designs. *Energy Environ. Sci.* **2020**, *13*, 977–985.
- (37) Yamanaka, I.; Hasegawa, S.; Otsuka, K. Partial Oxidation of Light Alkanes by Reductive Activated Oxygen over the (Pd-Black + VO(Ac)<sub>2</sub>/VGCF) Cathode of H<sub>2</sub>-O<sub>2</sub> Cell System at 298 K. *Appl. Catal., A* **2002**, *226* (1), 305–315.
- (38) Gao, J.; Xu, C. Q.; Hung, S. F.; Liu, W.; Cai, W.; Zeng, Z.; Jia, C.; Chen, H. M.; Xiao, H.; Li, J.; Huang, Y.; Liu, B. Breaking Long-Range Order in Iridium Oxide by Alkali Ion for Efficient Water Oxidation. *J. Am. Chem. Soc.* **2019**, *141*, 3014–3023.
- (39) Liang, Z.; Li, T.; Kim, M.; Asthagiri, A.; Weaver, J. F. Low-Temperature Activation of Methane on the IrO<sub>2</sub> (110) surface. *Science* **2017**, *356*, 299–303.